Jun Zhang participated in the Science Undergraduate Laboratory Internships (SULI) program at Brookhaven National Laboratory as a rising sophomore from Cornell University during the summer of 2005. His project involved characterizing the electric and magnetic properties of a doped nickelate compound that is closely related to the high temperature superconductors. During the summer of 2006, he worked in the SRF group at Cornell's Laboratory for Elementary-Particle Physics, where he helped set up, program and run a bead-pull apparatus that measures the electric axis of RF cavities. His work was used to optimize the beam quality inside the cavity. Jun plans on pursuing a PhD in Physics after he graduates from Cornell University.

Markus Hücker is an Associate Physicist in the Condensed Matter Physics & Materials Science Department at Brookhaven National Laboratory. He received a diploma (1994) and a Ph.D. (2000) in Physics, both from the University of Cologne, Germany. Prior to doing research at Brookhaven, he did postdoctoral research at the University of Paris, France. He earned the Karl Liebrecht Award, Faculty of Natural Sciences, from the University of Cologne, Germany, in 2000.

MAGNETIZATION, CHARGE TRANSPORT, AND STRIPE PHASES IN $Nd_{5/3}Sr_{1/3}NiO_{4+\delta}$ SINGLE CRYSTAL

JUN Z. ZHANG, MARKUS HÜCKER

ABSTRACT

Stripe phases, in which doped charges are localized along domain walls between antiferromagnetic insulating regions, provide a framework for the electronic structure of doped antiferromagnets such as the superconducting layered copper-oxides. Layered nickel-oxides, such as $Nd_{2-\chi}Sr_{\chi}NiO_4$, though non-superconducting, exhibit stripe phases in which charges are more localized, resulting in higher charge density modulation amplitudes than their cuprate analogs, thus are more amenable for experimental investigations. We study the magnetic and electric-transport properties of a $Nd_{5/3}Sr_{1/3}NiO_{4+\delta}$ single crystal by means of magnetic susceptibility, isothermal magnetization, and electric resistivity measurements. We observe a transition of the magnetic susceptibility with applied field parallel to the c-axis at $T \approx 15$ K, which is due to the long-range ordering of Nd^{3+} magnetic moments. A transition of the in-plane resistivity (ρ_{ab}) is observed at $T \approx 230$ K, which indicates the charge stripe ordering that has also been observed in $La_{2-\chi}Sr_{\chi}NiO_4$ at about the same temperature. The out-of-plane resistivity (ρ_c) exhibits a milder transition at $T \approx 200$ K. After the stripe phase transition takes place, the electronic transport exhibits variable range hopping behavior. The resistivity anisotropy (ρ_c/ρ_{ab}) shows a sharp drop at the ρ_{ab} transition temperature with decreasing temperature, which indicates the strong localization of charge carriers in the ab-plane as charge stripes become statically ordered and the system becomes less two-dimensional electronically. Our results are in support of the stripe phase picture of the electronic structure in layered metal-oxides.

INTRODUCTION

Since the discovery of high-temperature superconductivity in layered cuprates, the mechanism of charge transport in strongly correlated electronic systems has remained one of the most challenging problems in condensed matter physics. There is strong evidence that selforganized local inhomogeneities are responsible for the electrical properties of these systems. Stripe phases, in which charge carriers are confined to a single dimension between antiferromagnetic insulating regions, were theoretically predicted and experimentally observed in doped antiferromagnets by means of neutron scattering studies [1]. Extensive investigations of these materials in recent years have revealed that stripe correlations occur as a consequence of a complex interplay among spin, charge, and lattice degrees of freedom.

Isostructural nickelates, which remain insulating when doped with holes, are easier to study experimentally because they exhibit relatively static stripe order with higher charge density modulation compared with their cuprate analogs in which stripes are fluctuating. In recent years stripe correlations in $La_{2-\chi}Sr_{\chi}NiO_4$ have been studied extensively with many different experimental techniques such as neutron scattering, x-ray diffraction, thermal conductivity, NMR, specific heat, etc [2]. Nd substitution for La causes the lattice to change from the tetragonal structure to the orthorhombic structure, resulting in an anisotropic distortion of the NiO_2-planes. It has been

shown that stripes in $Nd_{2-\chi}Sr_{\chi}NiO_4$ align themselves in preferred direction, parallel to the [100] direction [3].

The goal of our research is to study the magnetic and electric-transport properties of $Nd_{5/3}Sr_{1/3}NiO_{4+\delta}$ by means of magnetization and electric resistivity measurements. Studies have shown that $La_{2-\chi}Sr_{\chi}NiO_4$ exhibits the most pronounced charge-ordering for a Sr doping of χ = 1/3 below 235 K [4]. Therefore we expect that $Nd_{2-\chi}Sr_{\chi}NiO_4$ with a Sr doping of χ = 1/3 would also exhibit the most distinct transitions in our experiments. Figure 1 shows the lattice structure of $Nd_{2-\chi}Sr_{\chi}NiO_4$ in its three structural phases, the high-temperature tetragonal (HTT) phase, the low-temperature orthorhombic (LTO) phase, and the low temperature tetragonal (LTT) phase [5].

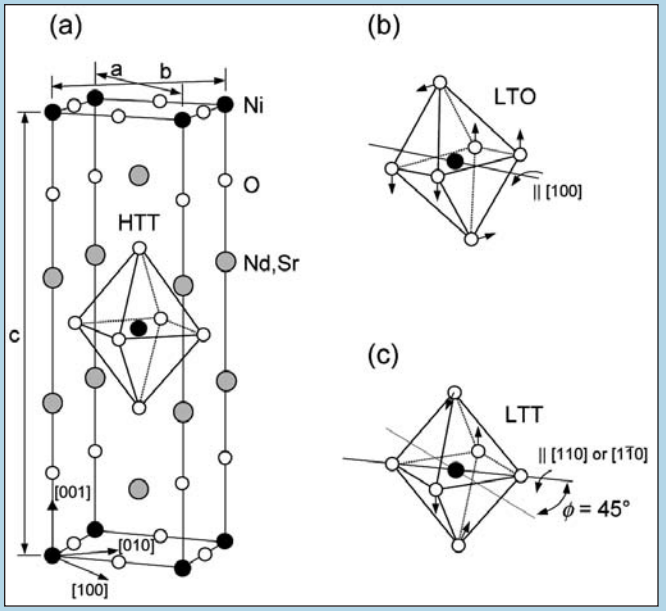

Figure 1. Lattice structure of $Nd_{2-\chi}Sr_{\chi}NiO_4$ and its three structural phases.

MATERIALS AND METHODS

Our single crystal sample of $Nd_{5/3}Sr_{1/3}NiO_{4+\delta}$ was grown by the Traveling-Solvent Floating-Zone (TSFZ) technique. Two pieces from the same grown crystal were used in our experiment. They were mounted with QuickCure acrylic on mounting blocks. We used the x-ray back-reflection Laue method to determine the crystallographic axes of both pieces and to orient them on a goniometer. Because our crystal has twinned domains in the ab-planes, we refer to the two in-plane axes as the ab1 and ab2 axes throughout this paper. The oriented crystals were then cut along the desired axes with a diamond blade sectioning machine. One sample with a flat surface parallel to the ab-plane (Figure 2(a)) was prepared for magnetization measurements so that we could easily orient its crystallographic axes with respect to the applied magnetic field. For the magnetization measurements, a bulky sample is preferred, to reduce the effects due to an anisotropic sample geometry. Two samples for resistivity measurements were shaped into thin bars (approx. 3.9 × 0.75 × 0.50 mm^3 and 2.0 × 0.70 × 0.50 mm^3) with each of their longest dimensions parallel to the ab1-axis and the c-axis, respectively.

Magnetic susceptibility and isothermal magnetization measurements were carried out using a superconducting quantum interference device (SQUID) magnetometer in a temperature range from 2 to 300 K with magnetic fields up to 7 T. For every measurement we took, the sample was first heated to high temperature and then zero-field-cooled to 2 K. The magnetic susceptibility was measured with magnetic field parallel to the ab1, ab2, and c directions with increasing as well as decreasing temperature. The mass of our as-prepared magnetization sample was determined to be m = 0.384 g using an electric balance. The molar susceptibility was calculated using the formula

$$\chi = \frac{\mu M}{Hm},$$

where μ is the measured magnetic moment, M is the molar mass of $Nd_{5/3}Sr_{1/3}NiO_{4+\delta}$ which is 2 about 392 g/mol, and H is the applied magnetic field strength. The isothermal magnetization was measured with field parallel to the c direction at 2 K, 5 K, 7.5 K, 10 K, etc. up to 30 K and with field parallel to the ab2 direction at 2 K.

The in-plane and out-of-plane resistivities (ρ_{ab} and ρ_c) were measured using the standard 4-terminal method. We used 0.002" pure platinum wires as contact leads, which were applied to polished sample surfaces with silver epoxies, followed by a heat treatment at 100°C in air for about an hour and then at 350°C in pure Ar gas for about two hours. This procedure was found to result in a very low contact resistance of the order of 1-10 Ω per lead. The Ar atmosphere was chosen to prevent oxygen annealing of the sample. The contacted sample for ρ_{ab} is shown in the photograph in Figure 2(b). The samples were then mounted on the probe with their leads soldered on the corresponding connectors. The probe was inserted in the magnet cryostat and connected to the resistance bridge which has an upper limit of 2 MΩ. The resistivity was calculated using the formula

$$\rho = \frac{RA}{L},$$

where R is the measured resistance, A is the cross-sectional area of the sample and L is the distance between the two voltage leads.

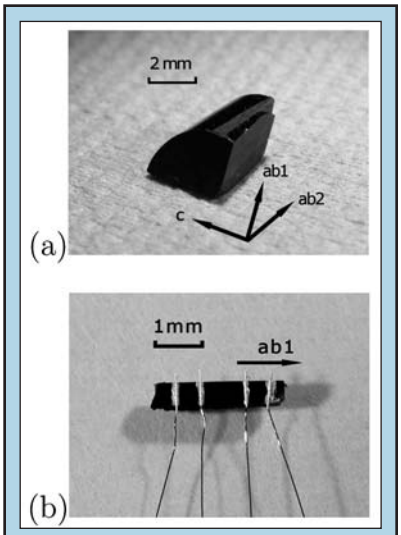

Figure 2. (a) The sample for susceptibility and isothermal magnetization measurements. (b) The ρ_{ab} sample with lead wires attached.

RESULTS AND DISCUSSION

Magnetic Susceptibility

Figure 3 shows the magnetic susceptibility $\chi(T)$ of $Nd_{5/3}Sr_{1/3}NiO_{4+\delta}$ for H = 1 T applied parallel to the three principal axes. The corresponding data will be referred to as χ_{ab1}, χ_{ab2}, and χ_c. For all the magnetic susceptibility measurements taken, measuring up and down with respect to temperature show no discrepancy within experimental error; therefore we only present the susceptibility data taken with increasing temperature. As indicated in Figure 3, χ_c shows an antiferromagnetic transition known as the Néel transition at $T_N \approx 15$ K, which is due to the long-range ordering of the Nd^{3+} moments. No apparent anisotropy in the NiO_2-planes is observed as we can see from the similar behaviors of χ_{ab1} and χ_{ab2}. However, the discrepancy between $\chi_{ab1,2}$ and χ_c suggests the presence of a crystal field perturbation.

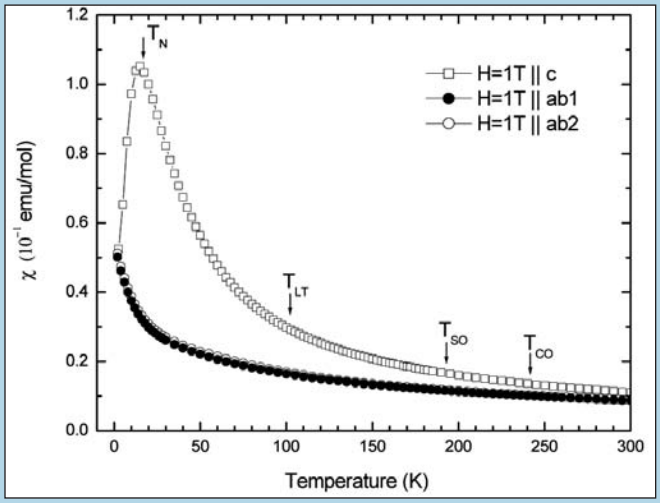

Figure 3. Temperature dependence of χ_{ab1}, χ_{ab2}, and χ_c. The expected transition temperatures are indicated.

Other than the Néel transition, we do not observe any other anomalies, for example, the transitions associated with the charge stripe and spin stripe orderings that have been observed in the susceptibility measurements on $La_{5/3}Sr_{1/3}NiO_4$ at about 240 K and 190 K, respectively [2]. The overall susceptibility can be attributed to the composition of different microscopic magnetic sources:

$$\chi_{NSNO} = \chi_{core} + \chi_{pauli} + \chi_{Ni} + \chi_{Nd},$$

where χ_{core} is the diamagnetic contribution of the closed electron shells, χ_{pauli} is the paramagnetic contribution of the conduction electrons, χ_{Ni} is the contribution due to Ni spins, and χ_{Nd} is the contribution due to the Nd moments. Both χ_{core} and χ_{pauli} are of the order of 10^{-4} emu/mol with opposite signs. χ_{Ni} is of the order of 10^{-3} emu/mol [4,6]. Therefore we think that the anomalies in the susceptibility due to charge stripe and spin stripe ordering are completely masked by the large contribution of the paramagnetic Nd^{3+} ions, which is of the order of 10^{-1} emu/mol (see Figure 3). The structural phase transition from the LTO phase to the LTT phase at T_{LT} = 100 K is also not apparent in the susceptibility data, which is unusual because in La_2NiO_4 [7] and $Nd_{1.8}Sr_{0.2}NiO_{3.72}$ [6] the transition leads to weak ferromagnetism.

The temperature dependence of the inverse susceptibility is plotted in Figure 4. The linear relationships at high temperature are indicated with lines fitted over $1/\chi_{ab2}$, and $1/\chi_c$. We see that the susceptibility clearly behaves according to the Curie-Weiss law [8]

$$\chi = \frac{C}{T - \theta},$$

where C is the Curie constant, in the high temperature regime (T > 100 K) for magnetic field applied parallel (χ_{ab1} and χ_{ab2}) as well as perpendicular (χ_c) to the NiO_2-planes. From the curve for $1/\chi_c$, the Weiss constant θ is approximated to be –10 K. The Curie-Weiss law predicts an antiferromagnetic transition near $T = |\theta| \approx 10$ K, which is indeed observed at TN ≈ 15 K. However, for field parallel to the ab-plane $1/\chi$ has a Weiss constant of about -100 K in which case the Curie-Weiss law is obviously a too simple model because it does not take into account the effects of the crystal electric field.

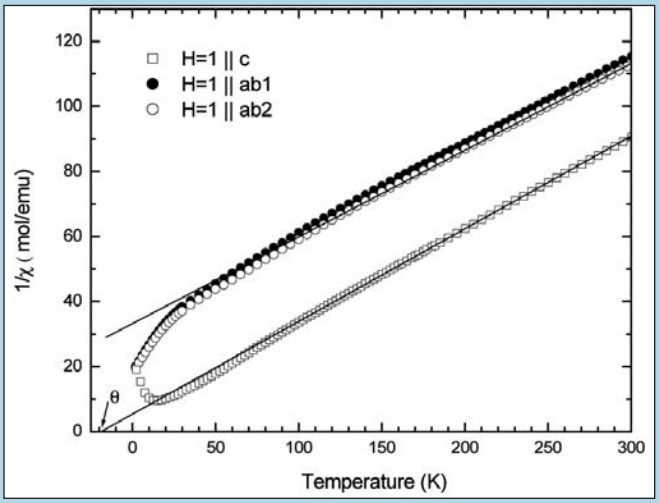

Figure 4. Temperature dependence of $1/\chi_{ab1}$, $1/\chi_{ab2}$, and $1/\chi_c$. Lines are fitted over $1/\chi_{ab2}$, and $1/\chi_c$ at high temperature.

Figure 5 shows the susceptibility for magnetic fields of various magnitudes applied parallel to the c-axis. We note that field strength has no noticeable effect on the susceptibility in the paramagnetic regime ($T > T_N$). However, a higher magnetic field tends to drive the Néel transition to lower temperature. Moreover, the susceptibility in higher magnetic field tends to decrease at a less rapid pace in the antiferromagnetic regime ($T > T_N$), indicating the suppression of the antiferromagnetic order by a uniform magnetic field. We have also measured the low field susceptibility (H = 20, 50, 100, 200 gauss) but again no additional anomalies are detected.

Isothermal Magnetization

Figure 6 shows the magnetization data $M(H)$ taken at T = 2 K, 5 K, 10 K, 15 K, 20 K, and 30 K with field parallel to the c-axis and at T = 2 K with field parallel to the ab2-axis. The measurements

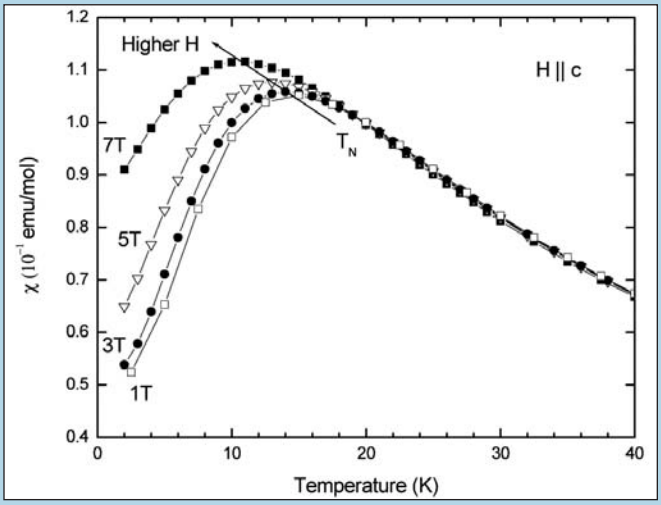

Figure 5. Temperature dependence of χ_c in different magnetic fields.

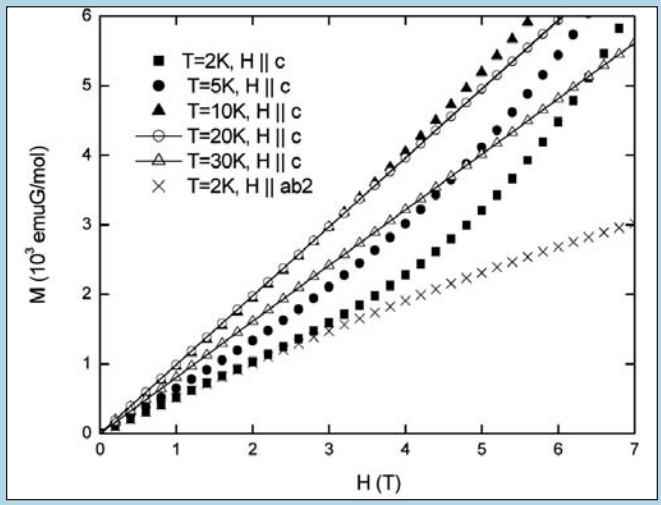

Figure 6. Field dependence of the magnetization at various temperatures with fields parallel to c-axis and ab2-axis.

were performed by increasing the field from H = 0 up to 7 T and then back to H = 0 at constant temperatures. The magnetization measurements at temperatures higher than T_N all exhibit linear field dependence, which is in agreement with the paramagnetic behavior at $T > T_N$ shown in Figure 3. Below T_N the field dependence of the magnetization is curving up, which indicates the onset of a magnetic transition. Unfortunately, we are limited by the 7 T capacity of our magnetometer, which prevents us from determining the critical field and the type of the magnetic transition.

Resistivity

Plotted in Figure 7 are the temperature dependence of the in-plane and out-of-plane resistivities (ρ_{ab} and ρ_c) with the vertical axis in the logarithmic scale and their temperature derivatives in the inset. Both ρ_{ab} and ρ_c clearly show insulating temperature dependence ($d\rho/dT < 0$) in the temperature range we studied. One feature in Figure 7 is that ρ_{ab} increases abruptly at about 230 K, indicative of a phase transition. The temperature derivative of $\log_{10} \rho$ in the

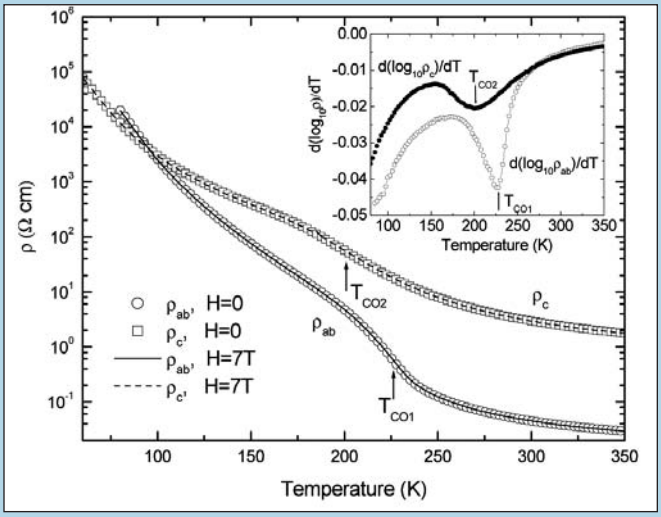

Figure 7. Temperature dependence of the in-plane and out-of-plane resistivities. The inset shows the temperature derivative of the resistivities.

inset of Figure 7 shows a sharp dip at $T_{CO1} \approx 228$ K, identifying the phase transition temperature. A similar transition in the in-plane resistivity of $La_{2-\chi}Sr_\chi NiO_4$ with $\chi = 1/3$ has also been observed and thought to be attributed to the segregation of doped holes to form the preferred charge-ordered state [4]. Neutron scattering and other experiments performed on $La_{2-\chi}Sr_\chi NiO_4$ showed conclusive results that the transition is due to the charge stripe ordering in the NiO_2-planes [9,10,11].

It is interesting to note that at $T_{CO2} \approx 200$ K ρ_c also exhibits a similar transition with a much milder feature. It is very likely that both transitions we see in ρ_{ab} and ρ_c are due to the charge stripe ordering. The fact that the charge stripe ordering takes place at two different temperatures may be attributed to the difference in the oxygen contents of our two samples. To verify this, we applied two more contact leads at the bottom of our ρ_c sample to measure the in-plane resistance across the bar-shaped sample and the out-of-plane resistance along the sample with the 2-terminal method using an electrometer, which has a build-in current source. To our surprise, the out-of-plane resistance shows a transition at 200 K, same as what we have observed before; however, the transition for the in-plane resistance is shifted down to 130 K (not shown in the figures). We suspect that the oxygen content of the sample has changed again; and it seems to affect only the in-plane resistivity. Further experiments are needed to determine the reason for the difference in the transition temperatures of ρ_{ab} and ρ_c. No anomalies due to the spin stripe transition and the LTO to LTT structural phase transition are observed in the resistivity.

We have also plotted ρ_{ab} and ρ_c on a logarithmic scale against $T^{-1/3}$ in Figure 8. The linear relationships below T_{CO1} and T_{CO2} suggest that the system's nonmetallic behavior is described within the variable range hopping (VRH) model as

$$\rho(T) \propto \exp\left[\left(\frac{T_0}{T}\right)^{\alpha}\right],$$

where T_0 is a measure of the localization of charges and the exponent α depends on the dimensionality of the VRH process. In our case

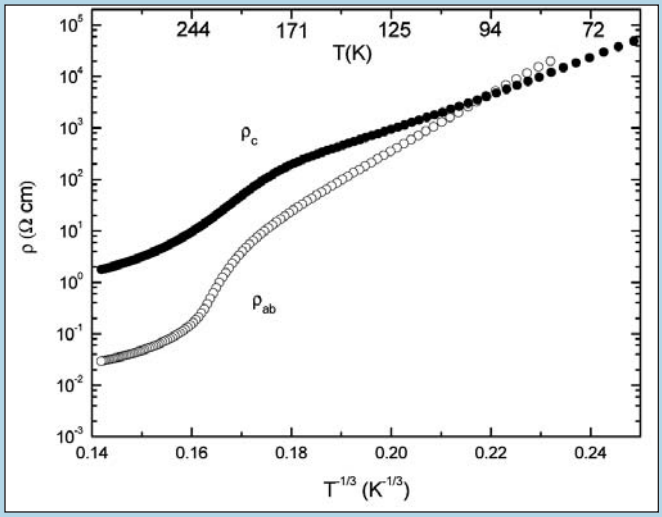

Figure 8. The in-plane and out-of-plane resistivities plotted against $T^{-1/3}$

ρ_{ab} and ρ_c are well described assuming α = 1/3 which corresponds to a two-dimensional hopping [12].

The resistivity anisotropy (ρ_c/ρ_{ab}) is calculated and shown in Figure 9. A strong temperature dependence of ρ_c/ρ_{ab} is noted. An abrupt decrease of ρ_c/ρ_{ab} is observed near the charge stripe ordering transition in ρ_{ab} at $T_{CO1} \approx 230$ K. When one compares Figure 9 to Figure 7, it becomes clear that the sudden drop in the resistivity anisotropy corresponds to the onset of the insulating behavior in ρ_{ab}. In other words, the rapid increase in ρ_{ab} causes the decrease of ρ_c/ρ_{ab} with decreasing temperature. The strong localization of charge carriers as charge stripes become statically ordered causes ρ_{ab} to rise more rapidly than ρ_c. As the more favorable in-plane charge transport mechanism breaks down, the system becomes a quasi-isotropic insulator. This can be seen in Figure 7 in which the two resistivities are of the same order of magnitude below 100 K. A similar phenomenon has also been observed in the cuprates [13].

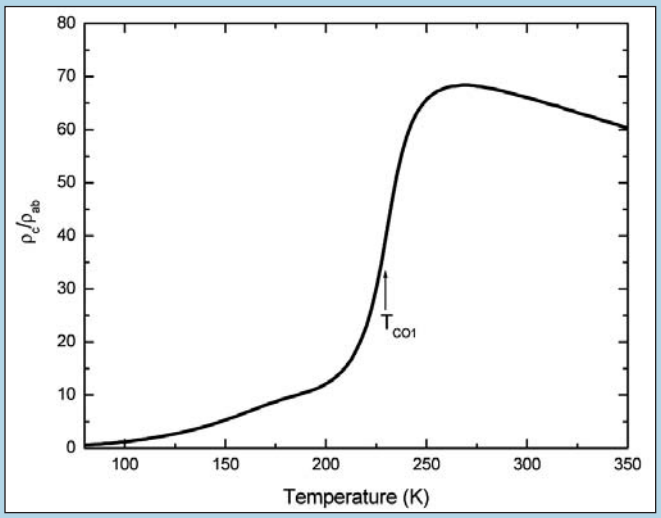

Figure 9. Temperature dependence of the resistivity anisotropy ratio ρ_c/ρ_{ab}.

CONCLUSION

Our research constitutes an important part of the characterization of $Nd_{2-\chi}Sr_\chi NiO_4$, a member of the nickelate family that has aroused considerable interest in the study of high temperature superconductivity. In this paper we have presented the measurements of the magnetization and of the resistivity of a $Nd_{5/3}Sr_{1/3}NiO_{4+\delta}$ single crystal. We observe an antiferromagnetic transition of magnetic susceptibility with applied field perpendicular to the NiO_2-planes at TN ≈ 15 K, which is due to the ordering of Nd^{3+} magnetic moments.

Charge stripe ordering is observed at $T_{CO1} \approx 230$ K in ρ_{ab} and $T_{CO2} \approx 200$ K in ρ_c. The discrepancy between T_{CO1} and T_{CO2} needs to be analyzed in future experiments. More suitable experimental techniques such as neutron scattering are needed to detect the spin stripe ordering and structural transitions in $Nd_{5/3}Sr_{1/3}NiO_{4+\delta}$. The resistivity anisotropy (ρ_c/ρ_{ab}) shows a sharp decrease at the ρ_{ab} transition temperature with decreasing temperature, which indicates the strong localization of charge carriers in the NiO_2-planes as charge stripe order takes place. Our results are in support of the stripe phase picture of the electronic structures in layered metal-oxides.

ACKNOWLEDGEMENTS

This research was conducted at the Brookhaven National Laboratory in Upton, NY. I would like to thank the U.S. Department of Energy, Office of Science for giving me the opportunity to participate in the SULI program. My sincere gratitude is given to my mentor Markus Hucker for his patient guidance and support. I would also like to thank Myron Strongin and John Tranquada for helpful discussions and assistance as well as Genda Gu for growing such a beautiful $Nd_{5/3}Sr_{1/3}NiO_{4+\delta}$ single crystal.

REFERENCES

[1] V. J. Emery, S. A. Kivelson, and J. M. Tranquada, "Stripe phases in high-temperature superconductors", *Proceedings of the National Academy of Sciences*, vol. 96, 8814 (1999).

[2] R. Klingeler, B. Büchner, S-W. Cheong, and M. Hücker, "Weak ferromagnetic spin and charge stripe order in $La_{5/3}Sr_{1/3}NiO_4$", *Physical Review B*, accepted for publication.

[3] M. Hücker, M. v. Zimmermann, S. Kiele, J. Geck, S. Bakehe, Revcolevschi, J. Hill, Büchner, and J. Tranquada, unpublished.

[4] S-W. Cheong, H. Y. Hwang, C. H. Chen, B. Batlogg, L. W. Rupp, Jr., and S. A. Carter, "Charge-ordered states in $(La,Sr)_2NiO_4$ for hole concentrations n_h = 1/3 and 1/2 ", *Physical Review B*, vol. 49, no. 10, 7088 (1994).

[5] M. Hücker, K. Chung, M. Chand, T. Vogt, J. M. Tranquada, and D. J. Buttrey, "Oxygen and strontium codoping of La_2NiO_4: Room-temperature phase diagrams", *Physical Review B*, vol. 70, no. 6, 064105 (2004).

[6] M. Medarde, J. Rodríguez-Carvajal, B. Martínez, X. Batlle, X. Obradors, "Magnetic ordering and spin reorientations in $Nd_{1.8}Sr_{0.2}NiO_{3.72}$", *Physical Review B*, vol. 49, no. 13, 9138 (1994).

[7] O. Friedt, "Preparation, characterization, and structure of $La_{2-\chi}Sr_\chi NiO_{4+\delta}$", diploma thesis 1998, University of Cologne, Germany.

[8] N. W. Ashcroft, N. D. Mermin, *Solid State Physics*, Philadelphia: Holt, Rinehart and Winston, 1976.

[9] S.-H. Lee and S-W. Cheong, "Melting of quasi-two-dimensional charge stripes in $La_{5/3}Sr_{1/3}NiO_4$ ", *Physical Review Letter*, 79, 2514 (1997)

[10] R. Kajimoto, K. Ishizaka, H. Yoshizawa, and Y. Tokura, "Spontaneous rearrangement of the checkerboard charge order to stripe order in $La_{1.5}Sr_{0.5}NiO_4$", *Physical Review B*, vol. 67, no. 1, 014511 (2003).

[11] A. Vigliante, M. von Zimmermann, J. R. Schneider, T. Frello, N. H. Andersen, J. Madsen, D. J. Buttrey, D. Gribbs, and J. M. Tranquada, "Detection of charge scattering associated with stripe order in $La_{1.775}Sr_{0.225}NiO_4$ by hard-x-ray diffraction", *Physical Review B*, vol 56, no. 13, 8248 (1997).

[12] M. Hücker, V. Kataev, J. Pommer, J. Harraβ, A. Hosni, C. Pflitsch, R. Gross, and B. Büchner, "Mobility of holes and suppression of antiferromagnetic order in $La_{2-\chi}Sr_\chi CuO_4$", *Physical Review B*, vol 59, no. 2, 50102 (1999).

[13] S. Komiya, Y. Ando, X. F. Sun, and A. N. Lavrov, "c-axis transport and resistivity anisotropy of lightly to moderately doped $La_{2-\chi}Sr_\chi CuO_4$ single crystals: Implications on the charge transport mechanism", *Physical Review B*, vol. 65, no. 21, 214535 (2002).